J. Am. Chem. Soc. 1992, 114, 91-98 91

This differs slightly from the structure of the S_4N_2 molecule produced from the decomposition of $(SN)_x$. The matrix infrared characterization of larger nitrogen sulfides invites more electronic structure calculations to test these bonding models.

Finally, the gas-phase reaction of N and S atoms at high dilution produced simple nitrogen sulfide species SN, N_2S, and NS_2 and not the larger sulfur nitride species S_2N_2 and S_4N_4 formed on evaporation of solid polymeric sulfur nitride.

Acknowledgment. We gratefully acknowledge financial support from NSF Grant CHE 88-20764 and the gift of a sulfur nitride sample from A. G. MacDiarmid.

Registry No. S, 7704-34-9; N_2, 7727-37-9; SN, 12033-56-6; NS_2, 12033-57-7; N_2S, 56400-02-3; NSS, 137122-34-0; NSSS, 88574-94-1; $SNNS_2$, 137122-35-1; NS–SN, 137122-36-2; NS_2^-, 91054-03-4; N_2S_4, 79796-33-1; ^{15}N, 14390-96-6; ^{32}S, 13981-57-2; ^{34}S, 13965-97-4; Ar, 7440-37-1.

An Interpretation of Organometallic Bond Dissociation Energies

Russell S. Drago,* Ngai M. Wong, and Donald C. Ferris

Contribution from the Department of Chemistry, University of Florida, Gainesville, Florida 32611. *Received May 17, 1991*

Abstract: Organometallic bond dissociation energies (BDE) are incorporated into the *E* and *C* model with excellent results. Since the data are consistent with gas-phase systems, the fit supports claims that the enthalpies are relatively free of solvation contributions. The organometallic catimers (fragments forming the positive end of the dipole) include $(CO)_5Mn^1$, $[\eta^5\text{-}(CH_3)_3SiC_5H_4]_3U^{IV}$–, $[\eta^5\text{-}C_5H_5](CO)_3Mo^{II}{}_5$–, $[\eta^5\text{-}C_5(CH_3)_5][P(CH_3)_3](H)Ir^{III}$–, $[\eta^5\text{-}C_5(CH_3)_5]_2(CH_3)_3CO]Th^{IV}$–, $[\eta^5\text{-}(C_5(CH_3)_5][P(CH_3)_3]_2Ru^{II}$–, $[(C_6H_5)_2PCH_2CH_2P(C_6H_5)_2](CH_3)Pt^{II}$–, $[\eta^5\text{-}C_5(CH_3)_5]_2Zr$–, and $^1/_2[\eta^5\text{-}[C_5(CH_3)_5]_2Sm]_2$–. The animers (fragments forming the negative end of the dipole) include organics, halogens, and inorganics. In addition to predicting and interpreting enthalpies, the resulting parameters for the radicals provide reactivity scales that can be used to interpret reactivity and physicochemical properties. Significant chemical insight results from the fit of the data to the *ECT* model. The parameters are used to reinterpret ^{19}F chemical shifts in $(F\text{-}Ph)Pt(P_2R_3)_2$–X, in terms of a σ-only Pt–X bond. The earlier interpretation is one of the classic examples used to support metal–ligand π-bonding interactions. Predicted bond energies are analyzed to indicate the metal properties that facilitate the CO insertion reaction. The analysis provides insights into the relative importance of electrostatic and covalent interactions. Further, the analysis shows that simply plotting the data of L_nM–X versus H–X gives an incomplete and potentially incorrect interpretation of the data. Another outcome of the analysis is that certain data points are brought into question as well as suggestions for key experiments needed to bring better insight into several systems.

Introduction

Organometallic chemists have had considerable success in the study of model reactions whose mechanisms provide insights regarding important fundamental steps in homogeneous and heterogeneous catalytic processes. As with the catalytic system, minor perturbations, e.g., change to another metal or ligand, often lead to dramatic changes in reactivity. Interest in obtaining a more fundamental understanding of this chemistry has led to a desire to understand the bonding energetics.[1] Such understanding is essential to improve and fine tune catalysts.

Measuring thermodynamic bond strengths or bond dissociation energies (BDE) for these systems is time consuming. It behooves us to extract the maximum amount of information and insight present in the data. An important component of understanding the data is being able to predict bond energies for new systems, thus eliminating the need for additional tedious measurements. Most attempts[1] to predict and interpret bond dissociation energies involve comparing the measured values for organometallic L_nM–X compounds with those for H–X, where X represents the negative end of the bond dipole and can be either an organic or inorganic group. This approach is of limited and uncertain utility because the relative importance of covalent and electrostatic bonding contributions usually varies in the L_nM–X and H–X compounds being compared. The complications introduced into such correlations from variation in the covalency have been discussed in detail for neutral donor–acceptor adducts[2] and for gas-phase ion–molecule correlations with proton affinities.[3]

In most correlations, systems that deviate provide the most interesting cases. For example, deviations from a linear plot of the dissociation energies of L_nM–X versus H–X are often attributed to π-back-bond stabilization or steric effects. These conclusions are open to question because deviations from these plots can arise from variation in the relative importance of covalent and electrostatic contributions to the bonding in the two systems plotted.[2] Another approach to explaining deviations in plots of H–X bond energies versus L_nM–X is to draw a second line for a new class of X groups. This is a sign that the covalent contribution to the bonding in L_nM is different from that in H.

When H–X bond energies are plotted versus L_nM–X bond energies, linear plots usually result when X is limited to a series of halides or to a series of alkyl compounds. When such plots are found, the conclusion that L_nM– and H– are similar is incorrect. For limited data sets, straight lines can be obtained even if L_nM– and H– are very different. In general, a plot of bond energies for two different systems provides little insight about the fragments plotted, and when deviations from the plot occur for

---

(1) (a) *Metal-Ligand Bonding Energetics in Organotransition Metal Compounds*; Marks, T. J., Ed.; Polyhedron Symposium in Print, 1988, Vol. 7. This is a series of articles by various contributors. (b) *Bonding Energetics in Organometallic Compounds*; Marks, T. J., Ed.; ACS Symposium Series 428; American Chemical Society: Washington, DC, 1990. (c) Simões, J. A. M.; Beauchamp, J. L. *Chem. Rev.* **1990**, *90*, 629. (d) *Handbook of Chemistry and Physics*, 71st ed.; Chemical Rubber Publishing Co.: Cleveland, 1985.

(2) Drago, R. S. *Inorg. Chem.* **1990**, *29*, 1379. Equation 2 becomes a linear equation for acids with the same C_A/E_A ratio $-\Delta H/E_A = E_AE_B/E_A + C_AC_B/E_A = E_B + kC_B$. Thus $-\Delta H = P_BE_A$ where P_B is a single parameter base scale equal to $E_B + kC_B$ and $k = C_A/E_A$. If the enthalpies of two acids are linear with the base parameter, they are linear to each other.

(3) Drago, R. S.; Ferris, D. C.; Wong, N. M. *J. Am. Chem. Soc.* **1990**, *112*, 8953.

0002-7863/92/1514-91$03.00/0 © 1992 American Chemical Society

a particular X functional group, they cannot be interpreted.

We have reported[4] success in the interpretation of bond dissociation energies with an ECT model:

$$-\Delta H_d = E_{cat}E_{an} + C_AC_B + T_{cat}R_{an} \qquad (1)$$

where "cat" refers to the catimer defined as the atom forming the positive end of the bond dipole while "an" refers to the animer, i.e., the atom forming the negative end of the dipole. E and C represent electrostatic and covalent bond forming tendencies, T the electron-transfer tendencies of the catimer, and R the electron-receptor tendencies of the animer. The energetics of forming a bond from two radicals is viewed as having electron transfer occur to produce the optimum covalent, electrostatic, and transfer bond strength components for the atoms or radicals involved. The transfer is driven in part by the tendencies of the animer to accept electron density and the catimer to transmit it. In a molecule, the extent of transfer is also facilitated by the increased Coulombic stabilization of the system that results when electron transfer occurs.

In view of the earlier success of the model,[3,4] we were encouraged to extend these correlations to the more complicated organometallic systems. The animer parameters determined from our earlier data set were employed in the interpretation of the organometallic systems. The new organometallic data led to a refinement of some of these parameters and the addition of new animers and catimers.

Results

The catimer and animer parameters empirically obtained from the least-squares fit of the enthalpy data are reported in Table I along with the parameters held fixed from the earlier report.[4] Those systems with limited bond energy data are marked tentative. They can be used with confidence to predict bond energies toward other animers or catimers only if their E, C, and T parameters are similar to those in the data set. The extension of these catimer parameters to other animers is not recommended, and any parameter interpretations based on their values is tentative. With the addition of new data, several of the parameters reported earlier were redetermined. The earlier and new data for any refined animer or catimer are combined in this fit; 184 enthalpies and 19 chemical shifts were solved for 91 unknowns. Of the 68 organometallic bond dissociation enthalpies, only 9 miss by values larger than experimental error. A molecular interpretation will be offered for most of these deviations in the Discussions. Table II contains the data fit (i.e., calculated and experimental values) of all the organometallic systems. It is surprising that so many of these organometallic systems are well behaved with our σ-bond model.[4c] Only nine show signs of steric effects, π-back-bond stabilization, or possibly errors in the data set. The excellent fit of the combined data from solution- and gas-phase studies, using some *ECT* parameters evaluated earlier from gas-phase data, supports the claims[5] that the solution bond dissociation energies employed are relatively free of solvation energies.

Table I. Catimer and Animer E, C, T Values for Use in Equation 1 to Predict Bond Energies

Catimer Parameters

formula^c	E_{cat}	C_{cat}	T_{cat}	$C/(E + T)$
$H-^a$	8.05	13.03	0.06	1.6
CH_3-^d	4.41	13.18^f	1.66	2.2
$C_2H_5-^e$	5.20	11.80	1.66	1.7
$C_6H_5CH_2-$	3.56^a	11.39	0.78	2.6
$(CO)_5Mn^I-^b$	3.16	5.45	14.89	0.30
$[\eta^5-(CH_3)_3SiC_5H_4]_3U^{IV}-$	2.14	5.84	21.51	0.25
$[\eta^5-C_5H_5)Mo(CO)_3-$	1.77	7.07	15.56	0.41
$[\eta^5-C_5(CH_3)_5][P(CH_3)_3](H)Ir^{III}-$	4.09	7.43	15.93	0.37
$[\eta^5-C_5(CH_3)_5]_2[(CH_3)_3CO]Th^{IV}-^b$	3.84	12.28	3.61	
$[\eta^5-(C_5(CH_3)_5[P(CH_3)_3]_2Ru^{II}-$	2.89	3.77	6.24	0.41
$[(C_6H_5)_2PCH_2CH_2P(C_6H_5)_2]-(CH_3)Pt^{II}-$	3.25	1.91	5.02	0.23
$^1/_2[[\eta-C_5(CH_3)_5]_2Sm]_2^-$	8.27	3.49	13.92	0.16
$[\eta-C_5(CH_3)_5]_2ZrR-$	6.56	7.57	19.74	0.34
$J_{CH_3}-^a$	−1.56	8.87	−2.42	
$I-^a$	3.48	6.18	1.93	
$Mn-^a$	3.59	2.70	25.16	
$C_6H_5-^a$	8.11	7.59	5.72	

Animer Parameters

formula	E	C	T
$-C(O)CH_3^b$	1.79	5.50	1.86
$-CH_2C_6H_5$	2.56	5.06	0.05^e
$-C_2H_5$	3.61	5.39	0.05^e
$-C_6H_5$	4.42	5.77	1.28
$-(CH_2)_3CH_3^b$	2.84	5.24	0.05^e
$-CH_3$	4.27	5.43	0.06
$-H^a$	2.23	6.60	0.97
$-F$	10.0^a	4.32	2.02
$-Cl$	6.69^f	3.78^f	2.11^f
$-Br^d$	5.81	3.16	1.83
$-I^d$	4.07	2.88	1.70
$-CH{=}CH_2$	8.55	2.87	0.88
$-CH_2Si(CH_3)_3^b$	3.44	5.52	0.05^e
$-OH$	7.15	4.54	1.54
$-C{\equiv}CC_6H_5^b$	5.92	6.30	4.44
$-CH_2C(O)CH_3^b$	2.40	6.05	0.05^e
$-OCH_3$	6.14	4.23	0.40
$-CN^a$	4.82	6.52	8.02
$-SH$	4.69	4.10	0.02^a
$-CCl_3^a$	3.64	5.10	2.70
$-CF_3^a$	3.76	5.84	3.70
$-NH_2^a$	5.29	4.82	0.39
$-N(CH_3)_2^b$	3.61	4.70	0.13
$-NO_2^b$	4.20	3.41	1.72
$-SCH_3$	3.82	4.40	1.84
$-OC_6H_5^b$	4.74	3.52	0.05^e

[a] Fixed from the earlier data set. [b] Tentative parameter. [c] The oxidation state indicated is that of the final compound formed. [d] Refit with new enthalpy[4b] (Luo, Y-R.; Benson, S. W. *J. Phys. Chem.* **1989**, *93*, 3305) data. [e] Parameter fixed to prevent it from going negative because only limited data are available. [f] In the course of running fits with varying weights to accomodate steric and π effects, this parameter did not change. It was held fixed in the final fit.

Discussion

Some Concepts Relevant to the Interpretation of Organometallic Bond Energies. Bond energies or bond dissociation energies that are relevant to a thermodynamic understanding of chemical reactivity are adiabatic enthalpies; i.e., the enthalpy compares the energy of the dissociated fragments in their ground-state configuration to that of the molecule. Usually, the perturbation made on the bonds to ancillary atoms (rearrangement and bond strength changes) when the ground-state radical reacts to form a bond is proportional to the animer–catimer bond strength. For example, the amount of change in the C–H bond strength and angles upon conversion of the planar methyl radical to a pyramidal CH_3–X depends on the C–X bond strength. This energy change is an inherent property of the ability of the radical to form a bond and is incorporated into the E, C, T parameters. Should the energetics of such rearrangements be larger for R_3C than for H_3C (and if this is the only factor that differs for the two systems), the energy difference would lead to larger *ECT* values for CH_3 and R_3C and to larger bond strengths for CH_3–X than R_3C–X. These geometry

---

(4) (a) Drago, R. S.; Wong, N. G.; Ferris, D. *J. Am. Chem. Soc.* **1991**, *113*, 1970. (b) Drago, R. S. *J. Phys. Chem.* In press. (c) A referee questioned whether the *ECT* parameters implicitly contain π-bond interactions in the parameters. Deviations would then have to be attributed to something else. Consider a C term doing this (the same arguments can be made for E and T). The π-acid, M, and π-base, X, parameters are then $(C_M + \pi_M)$ and $(C_X + \pi_X)$ and multiplication for C_AC_B gives $C_M\pi_X + C_X\pi_M + \pi_X\pi_Y$ as the π-stabilization energy. If M′ cannot π-bond and X′ cannot π-bond, $C_{M'}C_{X'}$ gives the covalent bond energy for M′X′. However, when M′ reacts with X, with no π-bonding possible, the predicted energy is too large by $C_{M'}\pi_X$, and when M reacts with X′, it is off by $\pi_MC_{X'}$. The π-bonding can only be accommodated by a separate term $(\pi_A\pi_B)$ because it is not present in all reactions of M or X. If systems are carefully selected to avoid π-stabilization, *ECT* is one of the best measures of this contribution. Unfortunately, not enough data are available to determine parameters for an independent $\pi_A\pi_B$ term.

(5) (a) Bryndza, H. E.; Fong, L. K.; Paciello, R. A.; Tam, W.; Bercaw, J. E. *J. Am. Chem. Soc.* **1986**, *108*, 7275 and ref 32 therein. (b) Schock, L. E.; Seyam, A. M.; Sabat, M.; Marks, T. J. *Polyhedron* **1988**, *7*, 1517.

Table II. Summary of Experimental and Calculated (Eq 1) Bond Energies for the Organometallic Systems in the Fit[a]

catimer	animer	expt	calc
$(CO)_5Mn^I$–	–CH_3CO	44.2	63.4
	–$CH_2C_6H_5$	30.8	36.4
	–C_6H_5	49.4	64.5
	–I	54.0	53.9
	–CH_3	44.7	44.0
	–H	58.6	57.4
η^5-$[(CH_3)_3SiC_5H_4]_3U^{IV}$–	–$CH_2C_6H_5$	35.6	36.1
	–$CH_2CH_2CH_2CH_3$	36.3	37.7
	–I	62.4	62.1
	–CH_3	44.8	42.2
	–$CH{=}CH_2$	53.3	53.9
	–$CH_2Si(CH_3)_3$	40.1	40.7
η^5-$[C_5(CH_3)_5](CO)_3Mo^{II}$–	–$CH_2C_6H_5$	32.0	41.1
	–CH_2CH_3	37.0	45.3
	–I	51.8	54.0
	–CH_3	47.0	46.9
	–H	66.0	65.7
	–Cl	72.4	71.4
	–Br	60.6	61.1
η^5-$[C_5(CH_3)_5][P(CH_3)_3](H)Ir^{III}$–	–C_6H_5	82.0	81.4
	–$CH_2CH_2CH_2CH_3$	52.0	51.3
	–I	64.0	65.1
	–CH_3	56.0	57.8
	–H	74.0	73.6
	–Cl	90.0	89.1
	–Br	76.0	76.4
	–$CH{=}CH_2$	71.0	70.2
η^5-$[C_5(CH_3)_5]_2[(CH_3)_3CO]Th^{IV}$–	–CH_2CH_3	78.9	80.2
	–C_6H_5	92.6	92.5
	–$CH_2CH_2CH_2CH_3$	75.6	75.4
	–CH_3	83.4	83.3
	–H	93.0	93.1
	–$CH_2Si(CH_3)_3$	82.3	81.1
η^5-$[C_5(CH_3)_5][P(CH_3)_3]_2Ru^{II}$–	–CH_2CH_3	29.0	31.1
	–C_6H_5	40.0	42.6
	–CH_3	34.0	33.2
	–H	40.0	37.4
	–$CH_2Si(CH_3)_3$	31.0	31.1
	–OH	48.9	47.2
	–$C{\equiv}CC_6H_5$	63.3	68.6
	–CH_2COCH_3	28.7	30.1
	–OCH_3	33.9	36.2
	–CN	63.0	88.6
	–SH	21.5	29.1
$[(C_6H_5)_2PCH_2CH_2P(C_6H_5)_2]$-$(CH_3)Pt^{II}$–	–CH_2CH_3	21.0	22.3
	–C_6H_5	31.0	31.9
	–CH_3	26.0	24.6
	–H	25.0	24.8
	–$CH_2Si(CH_3)_3$	22.0	22.0
	–OH	40.0	39.7
	–$C{\equiv}CC_6H_5$	54.3	53.6
	–CH_2COCH_3	20.0	19.6
	–OCH_3	24.7	30.1
	–CN	54.2	68.5
	–SH	21.5	23.2
$^1/_2[\eta^5$-$[C_5(CH_3)_5]_2Sm]_2^-$	–I	69.4	67.4
	–H	54.2	55.0
	–Cl	97.1	97.9
	–Br	83.6	84.6
	–$CH_2Si(CH_3)_3$	49.0	48.5
	–OCH_3	82.0	71.1
	–SCH_3	73.4	72.6
	–$N(CH_3)_2$	48.2	48.2
η^5-$[C_5(CH_3)_5]_2Zr$–	–I	81.0	82.1
	–CH_3	70.0	70.3
	–H	84.0	83.7
	–Cl	115.0	114.1
	–Br	98.0	98.2

[a] See supplementary material in the microfiche edition for the entire fit.

and bond-strength changes in ancillary bonds occur whenever any molecules or radicals react. The changes are *not* constant energy quantities that can be described as a constant promotion energy for the radical. It is important to keep this point in mind when interpreting trends in organometallic bond energies and spectroscopies.

Two important concepts that have been used in comparing bond dissociation energies will be considered in the context of the above discussion. Consider the case in which the unpaired bonding electron on a metal atom or radical exists in a degenerate set of orbitals containing other unpaired electrons. When a strong bond is formed localizing this bonding electron in the bonding interaction, the sizable exchange interaction involving this electron with the other unpaired electrons on the metal is lost. The importance of this effect in the interpretation of M–CH_3 and M–H bond strengths has been demonstrated.[7] If this energy loss is in direct proportion to the strength of the M–X bond, it will be incorporated into the *E*, *C*, and *T* parameters, causing them to be smaller than they would be in the absence of this exchange effect. If a constant promotion energy loss occurred as soon as any bond is formed (i.e., independent of the strength of the bond), the enthalpies would not fit *ECT* unless a constant energy, *W*, was added[6] to all the enthalpies that involve this metal species. The *ECT* data fit does not require that the loss of exchange energy in the relevant systems in this study be treated by a constant *W* approach. Therefore, the exchange energy loss is proportional to the bond strength. We shall consider it to be a factor in explaining the relative magnitudes of parameters but not use the concept to explain deviations from the fit. In nearly all the organometallic catimers studied, the metal fragment contains only one unpaired electron, and this contribution is negligible. However, in comparing the systems $Cp^*{}_2ThOC(CH_3)_3$–X and $Cp''{}_3U$–X (where $Cp^* = C_5(CH_3)_5^-$, $Cp'' = (CH_3)_3SiC_5H_4)^-$, and $Cp = C_5H_5^-$), the loss of exchange energy is probably a factor decreasing bond energies, i.e., *E*, *C*, *T* values, in the latter system.

The same arguments can be used to treat the energy lost from delocalization of an unpaired electron over a catimer or animer when it forms a bond. In this case, the bonding pair of electrons in the molecule may be delocalized over the molecule formed in direct proportion to the bond strength. There is no indication that a constant energy term is needed to account for those radicals in which the bonding electron is extensively delocalized. However, in order to interpret trends in bond strength, it should be realized that an electron that is extremely delocalized over an animer will lead to small *T* and *E* values with the delocalization energy loss on bond formation changing in proportion to the bond strength.

The points discussed above are important in comparing bond dissociation enthalpies and "bond enthalpy terms".[1c] The latter involve dissociation of a bond into fragments that have the same geometry as in the molecule (nonreorganized fragments). Thus, the "bond enthalpy term" is a "vertical" dissociation energy and the bond dissociation enthalpy an "adiabatic" dissociation energy. The latter is defined as the bond energy and is of most interest to synthetic chemists and solution thermodynamicists. The bond enthalpies are of importance in constructing cycles to extract bond dissociation enthalpies from gas-phase mass spectrometric type experiments, e.g., ICR, PES, etc.[1c] However, in a series of compounds L_nM–X, where L is a ligand, the geometry of the L_nM– fragment differs for different X substituents depending on the M–X bond strengths. Accordingly, the reorganization energy of L_nM upon M–X bond breaking is not a constant. Thus, the quantity that will be of sole concern in this manuscript is the adiabatic bond dissociation energy which for years has and will continue to be the chemist's measure of bond strength. Bond enthalpies are important in the interpretation of the influence of ancillary ligands on the magnitude of the *E*, *C*, *T* parameters.

The final concept to be evaluate is that of bond additivity. The usual form for the application of this idea in organometallic chemistry involves plotting H–X versus L_nM–X bond dissociation energies.[1c,5a] Energies for the unknown L_nM–X system[5] are then interpolated from known H–X bond dissociation energies. In the

---

(6) Drago, R. S. *Coord. Chem. Rev.* **1980**, *33*, 25 and references therein.

(7) (a) Mandich, M. L.; Halle, L. F.; Beauchamp, J. L. *J. Am. Chem. Soc.* **1984**, *106*, 4403. (b) Elkind, J. L.; Armentrout, P. B. *Inorg. Chem.* **1986**, *25*, 1078.

application of the E and C equation,

$$-\Delta H = E_A E_B + C_A C_B - W \qquad (2)$$

we have shown algebraically[2] that linear plots of formation enthalpies for one acceptor with a series of bases versus those of a second acceptor with the same bases arise only when the C_A/E_A ratio of the two acceptors are identical.[2] If plots are made for two acceptors using a limited series of donors with very similar C_B/E_B ratios, a straight-line plot may result but deviations will occur (or invalid predictions made) when a donor is studied whose C_B/E_B ratio varies from those employed in the plot.[2] The same arguments apply to plotting H–X bond energies versus those for L_nM–X with the problem further complicated by the contribution from the $T_{cat}R_{an}$ term. As can be seen in Table I, the $C/(E + T)$ ratio for the H catimer is 1.61. Those for the organometallic catimers are 0.41 ($CpMo(CO)_3$), 0.37 (Cp^*IrPMe_3H), 0.41 ($Cp^*Ru(PMe_3)_2$), 0.30 ($Mn(CO)_5$), 0.34 (Cp^*ZrR), 0.25 ($Cp''U$), 0.23 ($(DPPE)Pt(CH_3)$) (where DPPE = $(C_6H_5)_2P(CH_2)_2P(C_6H_5)_2$), and 0.15 ($Cp^*_2Sm$–X). (These abbreviations are expanded in Table I.) Thus, in principle, linear plots of L_nM–X versus H–X are not expected for most of these systems if a wide range of animers is employed. When linear plots are obtained employing a limited number of animers, prediction of new enthalpies from reported H–X versus L_nM–X plots must be limited to animers with C_B/E_{an} ratios and R_{an} values similar to those used in the plot. We shall further consider these plots in the discussion of the individual organometallic fragments.

General Trends in *E*, *C*, *T*, *R*. The qualitative bonding model evolving from these studies differs from the more familiar electronegativity model. As in standard bonding discussions, the E and C parameters correlate with charge/size ratios and HOMO–LUMO energy matches, respectively. The new feature of this model is the TR term. The T_{cat} parameters for the atomic catimers plot up smoothly with ionization energies, with a small T corresponding to a large ionization energy.[8] An exact correlation is not expected because ionization energy corresponds to removal of an electron from an isolated gaseous atom and T to fractional electron transfer from an atom in a molecule. In a similar fashion, R values for the animers parallel electron affinities with CN having a much larger R than expected on the basis of its electron affinity.

In the context of the ionic-covalent model, the TR term and EE term both contribute to ionicity (% ionic character = $(EE + TR)/\Delta H$), with CC being the familiar covalent term. In the case of sodium chloride, the T term makes a large contribution to the bond energy consistent with the low ionization energy of sodium and large electron affinity of chlorine. The transfer and electrostatic contributions account for 95% of the bond energy. In the case of HCl, the ionization energy of hydrogen is large and the transfer term small. The ionicity comes mainly from the EE term corresponding to the large Coulomb interaction arising from the small size of hydrogen. Thus, ionicity has two independent factors contributing to it, and these must be appreciated and considered separately to interpret bond strengths in terms of how ionicity arises. The electronegativity model attempts to treat the ionicity with one term which is a difference function ($23(\chi_F - \chi_X)^2$), and this does not reproduce the bond dissociation energies for a wide range of different systems very well.[4]

The T values of multiatomic catimers are influenced by the changes that occur in the bonding of the ancillary ligands when the catimer, L_nM, reacts with the animer to form the compound L_nM–X. The following order is observed for T: Cp''_3U^{IV}– > $Cp^*_2Zr^{IV}(X)$– > $Cp^*(Ph_3P)Ir^{III}(H)$– ~ $CpMo^{II}(CO)_3$– ~ $(CO)_5Mn^{I}$– ~ $Cp^*_2Sm^{III}$– > $Cp^*Ru^{II}(PMe_3)_2$– ~ $(DPPE)Pt^{II}(CH_3)$– > CH_3 > H–. Comparing the T value of Mn (25.2) with that of $Mn(CO)_5$ (14.9), the CO ligands are seen to lead to a decrease in T, suggesting an increased positive charge on the metal in $Mn(CO)_5$ than in the metal atom and/or a weaker Mn–CO bond in $Mn(CO)_5X$ than in the $-Mn(CO)_5$ animer. The stronger Mn–CO bond could arise from more effective π-back-bonding in the animer than in $Mn(CO)_5X$. The E values (3.59 versus 3.16) indicate a larger Coulomb interaction with the atom, but the large value suggests that the partial charge resulting from electron transfer when the $(CO)_5Mn$–X bond forms is largely localized on the metal of $Mn(CO)_5X$. The larger C for $Mn(CO)_5$ than Mn is consistent with a lower energy bonding MO, which is consistent with increased positive charge on the metal in the former. In summary, the five CO groups make relatively minor perturbations on the ECT values of the manganese atom in forming $Mn(CO)_5$ with the atom forming less covalent bonds. An interesting reversal in bond strengths is now appreciated. When X is a halogen, the bond to the manganese atom is stronger. When X is methyl, the increased covalency in $(CO)_5Mn$–CH_3 causes this bond to be stronger than that to the atom.

Next consider $Cp'_2Zr(X)$–X′. The large ionization energy for Zr(III) leading to Zr(IV) should lead to a T value close to zero for the atomic Zr^{3+} catimer. However, the bonding of Cp′ and X to zirconium decreases the energy of the metal HOMO, and stronger bonding of these ligands to Zr(IV) than to Zr(III) leads to a large transfer value. In all systems the Cp ligand is seen to facilitate transfer. Phosphine ligands have the opposite effect. The ruthenium system is one of the few complexes, another being $(DPPE)Pt(CH_3)$–X, containing two phosphine ligands. It appears as though better metal–ligand π-back-bonding in the low oxidation state catimer, L_nM, than in L_nM–X inhibits electron transfer in these complexes.

The relationship between E and T is interesting to consider. The E_{cat} trend is proportional to the charge/size ratio of the metal center. The charge depends upon the metal oxidation state and the donation of electron density to the metal by the ancillary ligands. This in turn depends on the covalency in the metal ancillary ligand bond. The T_{cat} has an opposite reaction to this property. A large charge/size ratio leads to a small T_{cat}. This is modified by electron donation from the ancillary ligands in the opposite way of E_{cat}. However, the charge formed as a consequence of the transfer may be localized on the metal or delocalized over the complex. The latter situation would lead to a large T and small E as in Cp''_3U. If the electron in the catimer is delocalized more effectively than the resulting positive charge is in the M–X compound, a small T and large E can result as in (DPPE)Pt. These effects cause T and E to be independent factors contributing to ionicity in these systems. The relationship of T to E will be discussed in considering the parameters of the individual ions.

The animer trends are also understood using the above arguments and lead to some interesting generalizations. The well-established parameters for hydrocarbons that form sp^3 or sp^2 bonds have C values of 5.5 ± 0.5 with the exception being the vinyl group ($C = 2.9$). Larger C values (~6.5) are observed for sp-bonded animers. As expected on the basis of energy match, nitrogen (sp^2) animers have smaller C values than analogous carbon animers, and oxygen (sp^2) lower than nitrogen. An E trend, in the opposite direction, is also expected and observed from energy match considerations. Overlap leads to a slightly smaller C value for –SH than OH. The trend in the E values for the saturated aliphatic carbon animers parallels the size. In comparison to the saturated carbon animers, the vinyl group and phenyl sp^2 carbons have large electrostatic contributions. The E trend O > N > C for animers of comparable size is that expected on the basis of the ionic character of the bonds. The receptor values are ~0.1 for carbon animers that form sp^3 bonds, increasing to about 1 for those that form sp^2 bonds and increasing for sp bonds to 5 for acetylide and 8 for cyanide. The trend in the E values of H and CH_3 animers does not follow charge–size consideration and suggests the electron density transferred to the CH_3 animer residues on the carbon in the orbital pointed at the catimer. This leads to a smaller effective size for the CH_3 animer. The trends in the halides and hydroxide have been discussed earlier.[4] In ascertaining the ionic character of a bond, both E and R operate in a synergistic way to facilitate electron transfer to the animer.

---

[8] The exception involves Mg which has a pair of electrons in an s orbital. This sytem can be viewed as having reduced ECT values because it involves forming a weaker three-electron bond to the animer.

$Cp^*Ir[P(CH_3)_3](H)$–X. This system[1a,9] is very well defined. Data for X = Cl, Br, I, H, and CH_3 were used in our earlier fit.[4] Adding additional data for X = C_6H_5–, $CH_3(CH_2)_3$–, and CH_2=CH– leads to refined parameters for this system that have changed only slightly from the earlier data fit. All animers are fit well, indicating that the Ir–X bond in all these systems is a normal σ bond. There is no indication of steric effects or π-back-bond stabilization in the reported systems.

The large T for a catimer with a phosphine ancillary ligand (vide infra) suggests that not much metal–ligand π-back-bonding exists in the catimer or the higher metal oxidation state compounds M–X. This catimer has a larger C/E ratio than hydrogen, but a large transfer contribution leads to a smaller $C/(E + T)$ ratio. The larger $C/(E + T)$ ratio of hydrogen than $Cp^*Ir(PMe_3)H$ (1.61 versus 0.37) does not mean that hydrogen will always form the more covalent bond. The ratios only provide a rough guide, and the products of the animer and catimer interaction must be calculated for a direct comparison. The percent covalent character in HCl is 48% compared to 32% for L_nIr–X. On the other hand, the H–CH_3 bond is 67% covalent and Ir–CH_3 bond is 69% covalent. This type of reversal in ionicity as the animer varies is a feature accommodated by having both a transfer and Coulomb term to describe ionicity.

In this system the M–H bond is calculated to be ~15 kcal mol^{-1} more stable than M–CH_3. The transfer term contributes 14 kcal mol^{-1} and the covalent term ~9 kcal mol^{-1} to hydride stability. The electrostatic term stabilizes CH_3 by ~8 kcal mol^{-1} over the hydride.

$Mn(CO)_5$–X and $CpMo(CO)_3$–X. The $Mn(CO)_5$–X data[1c,10] is not fit well by *ECT*. It appears that V-shaped animers (those that contain two second-row or higher atoms attached to the animer atom) undergo steric repulsion with the carbonyl groups of the $Mn(CO)_5$ fragment. Consider the atoms attached directly to the metal as forming a sphere and those attached directly to these atoms as forming a second sphere, etc. Steric effects can arise in any sphere being most common in the first and second spheres. For the phenyl radical, the carbon is small and first-sphere repulsions are not significant. However, the ortho carbons and hydrogens attached to the ortho carbon are involved in second-sphere repulsions with the oxygens of the $Mn(CO)_5$ fragment. For acetyl, the oxygen and methyl group are involved in second-sphere repulsions. Second-sphere steric problems are also suggested for the benzyl group. Based on limited data, a C of 5.45 and an E of 3.16 results. The T value is large but reduced to 15 from the value of 25 for the manganese atom. The relatively large E value of 3.2 compared to 3.5 for the manganese atom indicates that most of the charge formed from electron transfer is localized on the manganese. The CO ligands are relatively innocent ancillary ligands which mainly function in bonding to produce a better bonding orbital for $Mn(CO)_5$ than exists in Mn atoms. As a consequence, the $Mn(CO)_5$–CH_3 bond is stronger than Mn–CH_3, but the more electrostatic Mn–I bond is stronger than $Mn(CO)_5$–I.

The complex[11] $CpMo(CO)_3$– has a large C (7.1), a small E (1.77), and a T value of 15.6. A two oxidation state metal is expected to have less transfer than a one oxidation state, e.g., $Mn(CO)_5$. Comparable values in these two catimers indicate the very sizable perturbations made on the free metal by coordination of the cyclopentadiene group. The metal partial positive charge is reduced and greater covalency in the metal–Cp bond in the higher oxidation state Mo(II) compound than in the Mo(I) catimer facilitates transfer. The small E indicates that the charge produced from transfer is delocalized over the catimer. Second-sphere, steric effects are evident in this system for the animers benzyl and ethyl.

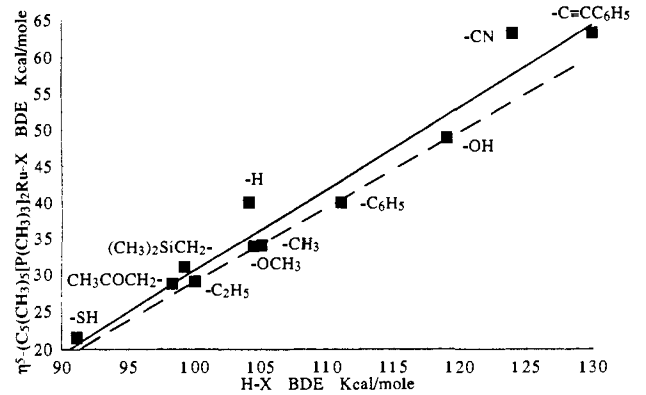

Figure 1. Plot of the HX bond dissociation energy vs the η^5-$C_5(CH_3)_5$-$[P(CH_3)_3]_2Ru^{II}$–X bond dissociation energy.

$Cp^*Ru(PMe_3)_2$–X. The data for this system fit E, C, and T well considering two enthalpies (CN and SH) are only estimates. If the CN animer and H are given equal weight, the M–H bond energy misses by 5 kcal mol^{-1}. If the M–H bond energy is reproduced, the experimental M–CN bond energy is lower than that calculated. We have weighted the fit to reproduce the M–H bond energy because the reported M–CN and M–SH values are only lower limits. It is of interest to compare this ruthenium system[5a] with the isoelectronic and geometrically similar $Cp^*Ir[PMe_3]H$–X compound. The oxidation state of the metal is one unit lower in the former, making the partial charge on the metal smaller, decreasing its charge/size ratio and the E value. The lower oxidation state for ruthenium leads to a higher energy HOMO for the catimer and a smaller C number. The larger value of T for the higher oxidation state $Cp^*Ir(PMe_3)H$ compared to the ruthenium system is attributed to the ability of the ancillary hydride and phosphine ligands to facilitate transfer by forming a stronger σ bond to the metal in the iridium–X compound than in the catimer. More effective π-back-bonding from ruthenium to phosphine in the animer than exists in the larger, higher oxidation state iridium animer could also be a factor inhibiting transfer in $Cp^*Ru(PMe_3)_2$. Data on a wider range of compounds is needed to better define the *ECT* bonding patterns from the ancillary ligands. It is interesting to note that all the E, C, and T parameters of $Cp^*Ru(PMe_3)_2$ are roughly about one-half those of $Cp^*Ir(PMe_3)H$–. On a percentage basis, the bonding is similar in the two compounds.

Figure 1 is a plot of the bond formation energies of H–X versus those for $Cp^*Ru(PMe_3)_2X$. The solid line is the least-squares line for all the points and the dashed line connects C_2H_5, CH_3, C_6H_5, OCH_3, and OH. The fact that nine of the animers studied behave similarly toward hydrogen and Cp*Ru (i.e., the bond energies differ for each X by 69 ± 2 kcal mol^{-1}) leaves two enthalpies (M–H and M–CN) to distinguish the *ECT* differences. The literature interpretation of these data draws the best line through these points, interprets the CN deviation to π-back-bonding, suggests a new line may exist for "softer" third-row donors, and suggests $Cp^*(PMe_3)_2Ru$–X bond energies can be interpolated from the H–X bond energies. The nonzero intercept in this plot is not addressed. On the other hand, the *ECT* model suggests that the experimental CN σ-bond energy and the sulfur σ-bond energy are too low (both are reported to be a lower limit), there is no evidence for π-back-bonding, and except for alkyl animers it would be very dangerous to estimate metal–X bond energies for this system from the H–X bond energies. Unfortunately, the choice between the two interpretations is based on two enthalpies, Ru–H and RuCN. However, the *ECT* model and the H–X interpolation can be used to predict bond energies for $Cp^*(PMe_3)_2Ru$–X for X = F, Cl, Br, and I. The results are 58 vs 67, 47 vs 34, 40 vs 12, and 34 vs 1 for the *ECT* and the H–X model, respectively. *Thus, measurements on these systems will distinguish the two interpretations of the bond dissociation energies.*

$[(C_6H_5)_2PCH_2CH_2P(C_6H_5)_2]PtCH_3$–X. This system[5a] has a C value of 3.25, an E of 1.91, and a T of 5.02 being the least covalent of the late transition metal systems studied. The low T value of 5.02 is similar to that for $Cp^*Ru(PMe_3)_2$–X for similar

---

[9] Nolan, S. P.; Hoff, C. D.; Stoutland, P. O.; Newman, L. J.; Buchann, J. M.; Bergman, R. G.; Yang, G. K.; Peters, K. S. *J. Am. Chem. Soc.* **1987**, *109*, 3143.

[10] Connor, J. A., et al. *Organometallics* **1982**, *1*, 1166.

[11] Nolan, S. P.; Lopez de la Vega, R.; Mukerjee, S. L.; Gonzalez, A. A.; Zhang, K.; Hoff, C. D. *Polyhedron* **1988**, *7*, 1491 and references therein.

reasons. The E values are comparable in the platinum system and ruthenium systems, and the smaller C corresponds to a higher HOMO energy and poorer overlap for a third-row metal ion compared to a second-row metal ion. Both the –CN and –SH bond energies are reported as lower limits and weighted accordingly in the fit. The *ECT* predicted enthalpies are 14 and 2 kcal mol^{-1} higher than the lower limit reported. The reported BDE for $-OCH_3$ is poorly fit and unreasonable when compared to hydroxyl.

The bond dissociation energies plotted versus those of the analogous H–X compounds produce results that are similar to those of the $Cp^*Ru(PMe_3)_2$ except the H animer now falls on the line while the CN and S–H systems fall off the line. Again the bond dissociation energy of HI would predict a zero bond dissociation energy for $(DPPE)Pt(CH_3)-I$. The *ECT* prediction of 27 kcal mol^{-1} is more reasonable. In the *ECT* fit, all systems studied are well behaved. The CN and SH bond energies fit well and the σ bond strengths are predicted to be higher than those estimated from HX. There is no indication of metal–ligand π-back-bond stabilization in the CN system as proposed[1a,11] earlier from the H–X analysis which underestimates the σ-bond strength. It is interesting to note that all bond energies for this system are 8 or more kcal mol^{-1} less than for $Cp^*Ru(P(CH_3))_2-X$ except for the –SH animer. This supports our prediction of a BDE ~29 kcal mol^{-1} for $Cp^*Ru[P(CH_3)_3]_2-SH$ and is consistent with the literature assignment of a lower limit to the value reported.

The HX bond dissociation energy should be used to predict L_nM-X dissociation energies only for alkyl groups or other animers with comparable C, E, and R values. Other systems may correlate, e.g., OH, if there is a fortuitous combination of E, C, and transfer contributions, but reliable predictions cannot be made. The *ECT* prediction is the recommended alternative because the parameters for this catimer are reasonably well defined.

η^5-Cp″$_3$U–X and η^5-Cp*Th[OC(CH$_3$)$_3$]–X. The literature compilations (see refs 1a and 1c) on the η^5-Cp''_3U-X system vary slightly depending on the choice of $D(R-I)$ values employed in the calculations. The best fit was obtained with the compilation of Simões and Beauchamp.[1c] This system[1a,c,12] is fairly well defined and well behaved with no indication of steric effects or other unusual bonding interactions in the systems studied. Such effects have been proposed to account for the significantly lower bond dissociation energies of this system (which employs absolute values) compared to Cp^*_2UCl-R and other systems (which are anchored to an estimated U–O bond energy). We calculate a σ-bond dissociation energy for the η^5-Cp''_3U-OCH_3 system of 46 kcal mol^{-1}. Even allowing for additional oxygen-to-metal π-stabilization (which should be less than the 11 kcal mol^{-1} observed for $Cp^*_2SmOCH_3$), this value is considerably below that used to anchor several of the uranium systems. This probably accounts for the large differences in the absolute values for η^5-Cp''_3U-X and the bond strength of other uranium systems.

The thorium system is poorly defined because all of the data involve similar animers. If a Th–I bond energy of 75 kcal mol^{-1} is assumed, a data fit is obtained in which the phenyl system misses by 8 kcal mol^{-1} (steric effects?) giving E, C, and T parameters of 6, 11, and 11, respectively. Thus a good deal of uncertainty exists for this system. The parameters in Table I and the above parameters predict a $Th-OCH_3$ σ-bond energy of 77 and 87 kcal mol^{-1}, respectively. Both values are considerably lower than literature estimates.

Cp*$_2$Sm–X. The Cp^*_2Sm-X compounds[13] are well behaved even though the products and reactants are associated. The excellent fit of *n*-PrS– ($-S-CH_3$ parameters used) and $N(CH_3)_2$ indicates that there is little ligand-to-metal π-stabilization in these compounds. The 11-kcal mol^{-1} deviation of the value calculated for $-OC(CH_3)_3$ (using OCH_3 parameters) suggests some π-stabilization. It is suprising that $-OC(CH_3)_3$ is stabilized but $-N(CH_3)_2$ is not. This could result from the tentative nature of the $N(CH_3)_2$ parameters. Unfortunately, only one Cp^*_2Sm-X compound is reported with a metal–carbon bond, and this involves the animer $-CH[Si(CH_3)_3]_2$. Since the parameters for this animer are not available, the enthalpy for bonding to $-CH_2Si(CH_3)_3$ is estimated by multiplying the measured enthalpy for $CH[Si(CH_3)_3]_2$ by the ratio of $-\Delta H\{(CH_3)_3SiCH_2-H\}/-\Delta H\{(CH_3)Si]_2CH-H\}$. The dat fit shows this catimer to be the most electrostatic organometallic system studied with a $C/(E + T)$ ratio of 0.15.

Cp*$_2$ZrR–. The reported data for this system are a mix of various R substituents including halides. In spite of this, the data fit is good. The T_{cat} value is similar to the uranium complex with C_A larger and E_{cat} much larger. The large E value also facilitates electron transfer and suggests a larger charge/size ratio at the metal center in the zirconium system. The $-N(CH_3)_2$ and *t*-BuO– dissociation energies are poorly fit. The comparison of the measured value of 85 kcal mol^{-1} to the calculated value of 62 kcal mol^{-1} for the dissociation energy of $Zr-N(CH_3)_3$ suggests extensive ligand-to-metal π-bonding. This is supported by the difference in the measured dissociation energy of the *t*-BuO–Zr (104 kcal mol^{-1}) compared to the calculated value of the analogous system $Zr-OCH_3$ (80 kcal mol^{-1}).

General Trends in Organometallic Reactivity. Several insights regarding the reactivity of these organometallic compounds can be inferred from reported and *ECT* estimated enthalpies. With the E_{an}, C_B, and R_{an} value of phenyl all larger than CH_3, the $L_nM-C_6H_5$ bond dissociation energy is and will always be slightly larger than L_nM-CH_3 unless a steric effect is operative. The prediction is quite different for L_nM-H and L_nM-CH_3 bond dissociation energies. Catimers with a large transfer terms tend to form stronger bonds to hydrogen than methyl. The more covalent catimers with a small transfer term will also bond more strongly to hydrogen. In all catimer systems where the C/E ratio is ≥ 2 and T is ≥ 3, the M–H bond energy will be larger than the $M-CH_3$ bond energy. Those systems with a small C/E ratio and a small transfer term will form bonds of comparable strength to H and CH_3 (e.g., $(DPPE)PtCH_3-$) or produce systems where the methyl is bound stronger than hydrogen. The large E and moderate T of $[Cp^*_2Sm]_2$ leads to a predicted value of 54 kcal mol^{-1} for the methyl derivative compared to 55 kcal mol^{-1} for hydrogen.

Our next concern is with the hydrolytic stability of the alkyl and hydride derivatives. It is tempting to attribute the instability of Cp''_3U-R compared to $(DPPE)PtCH_3-X$ (where X = H or CH_3) to an ionic metal alkyl or metal hydride bond in the former. The *ECT* model assesses 75% covalency in the uranium–methyl bond and 42% covalency in the platinum–methyl. The hydrolytic instability of the uranium is attributed to the strong U–OH bond and the hydrolytic stability of the platinum complex to the weak Pt–OH bond. The reaction:

$$Pt-CH_3 + H-OH \rightarrow Pt-OH + CH_4$$

is predicted to be near thermoneutral. The large Cp_3U-OH (>74 kcal mol^{-1}) bond energy compared to about 45 for $U-CH_3$ makes the reaction

$$Cp_3U-R + H_2O \rightarrow Cp_3U-OH + RH \qquad (3)$$

very exothermic.

The ionicity in the $M-CH_3$ metal carbon bond varies from 66% for the samarium compound to 18% for $CpMo(CO)_3$. The order of decreasing ionic character to methyl is $Cp^*_2Sm > DPPE(CH_3)Pt- > Cp''_3U- > Cp^*_2(R)Zr > -Mn(CO)_5 > Cp^*Ir(PMe_3)(H) \sim Cp^*Ru(PMe_3)_2 \sim CpMo(CO)_3$.

In comparing the *ECT* parameters of CH_3 and OH, it can be seen that the hydroxide will be more stable toward those catimers that have large E and large T values. When the OH compound, L_nM-OH, is about 15 kcal mol^{-1} more stable than the methyl derivative, the hydrolysis reaction will be thermoneutral. Of course, the free energy of eq 3 in aqueous solution has many other factors contributing to it. Product volatility also drives reactions to completion. The above considerations show that bond energies

---

[12] Bruno, J. W.; Stecher, H. A.; Morss, L. R.; Sonnenberger, D. C.; Marks, T. J. *J. Am. Chem. Soc.* **1986**, *108*, 7275.

[13] Nolan, S. P.; Stern, D. P.; Marks, T. J. *J. Am. Chem. Soc.* **1989**, *111*, 7844.

provide a large component of the observed reactivity and illustrate the pitfalls of trying to infer ionic character from chemical reactivity.

The carbonyl insertion reaction is of considerable importance in catalytic CO reduction chemistry. The reader is referred to an excellent review by Wayland et al.[14] demonstrating the insights provided, in systems of this sort, by thermodynamic considerations. The basic reaction involves:

$$\mathrm{CO} + \mathrm{M(CO)_5CH_3} \rightarrow \mathrm{(CO)_5M{-}C(O)CH_3} \qquad (4)$$

The energetics involves dissociating a metal–carbon bond, forming a metal–acetyl bond, and forming an acetyl radical from $CH_3^{\bullet}$ and CO. The bond energy for bonding acetyl to a metal compared to that for bonding a methyl radical depends upon the difference in the E_{an}, C_B, and T_{an} values of acetyl and methyl, i.e.

$$\Delta\Delta H = E_{cat}\Delta E_{an} + C_A\Delta C_B + T_{cat}\Delta R_{an} \qquad (5)$$

Using the data in Table I, one calculates $\Delta E = -2.5$, $\Delta C = \sim 0.1$, and $\Delta R = 1.8$ where Δ is the difference in the $MCOCH_3$–MCH_3 parameters. Since the heat of formation of acetyl is a constant and if we assume the bond energy of CO bonding to $M(CO)_4(CH_3)(CO)$ is comparable to that in $M(CO)_4(CH)_3$, the insertion reaction will be favored in complexes that have a large transfer term and a small E_{cat} term. The greater electron transfer into acetyl than methyl drives this reaction. Complexes should be used with ligands that facilitate transfer and delocalize the positive charge off the metal center of the catimer. Systems in which steric effects exist for the bound acetyl will have an energy contribution that is unfavorable for insertion. Steric problems are expected to contribute to the facile conversion of coordinated benzoyl (PhC═O) to $M{-}C_6H_5$ + CO. Calculations of ΔE, ΔC, and ΔT values for acetyl (for RCO) and ethyl as well as acetyl and benzyl produce the observed order[15] of CO insertion $C_2H_5 > PhCH_2 > CH_3$.

Data are not available to determine *ECT* for formyl, but with the bond dissociation energy of H–COH and $H{-}COCH_3$ being the same (87 kcal mol^{-1}), within experimental error, we shall assume similar *E*, *C*, *T* values as was done above. This leads to $\Delta E = -0.4$, $\Delta C = -1.1$, and $\Delta T = 0.9$ with $\Delta = MC(O)H - MH$. Again the transfer term drives the insertion to produce a σ-bonded η^1, with Cp''_3U and Cp_2Sm being the more favorable cases for reaction. However, with both ΔE and ΔC negative and a smaller ΔT, the η^1 formyl will never form as readily as acetyl. To facilitate a catalytic reaction, alternate bonding modes for formyl, possibly η^2, should be sought. The η^2 mode is reported[16] for CO insertion into the thorium hydride bond. The reaction can also be facilitated in a noncatalytic mode by replacing the coordination position vacated by H migration with a strong base instead of another CO.

Spectral Shift Interpretations. In earlier articles,[6] we have shown that a spectral shift, $\Delta\chi$, can be substituted for $-\Delta H$ in eq 2. A successful fit of the data indicates that the same factors that influence bond strengths for a catimer or animer also influence spectroscopy though not necessarily with the same weighting of the electrostatic and covalent contributions. In this context, it was of interest to examine some classic data bearing on the electronic character of metal anion bonds. Table III lists ^{19}F shielding parameters for a series of bis(triethylphosphine)-*m*-fluorophenylplatinum(II) complexes. In a usual fit, the animer parameters reported in Table I are substituted into eq 6:

$$\Delta\chi = \text{“}E_{cat}\text{”}E_{an} + \text{“}C_A\text{”}C_B + \text{“}T_{cat}\text{”}R_{an} \qquad (6)$$

and the resulting series of simultaneous equations solved for “E_{cat}”, “C_A”, and “T_{cat}”, where the quotes indicate parameters for spectral data. In this instance, the ^{19}F shift of the catimer is not known; a $\Delta\chi$ (^{19}F PtX–catimer) cannot be calculated so $\Delta\Delta\chi(\Delta\zeta^{19}F)$ is defined as the chemical shift difference, δ, of $L_nPtX{-}L_nPtI$; and ΔC_B, ΔE_{an}, and ΔT_{an}, determined by subtracting the iodide parameter from the reported *X* parameters, are used in the fit of $\Delta\Delta\chi$ to eq 6. The calculated $\delta^{19}F$, is then obtained by adding the $\delta^{19}F$ value of L_nPtI to that calculated for $\Delta\delta^{19}F$ in the fit. An excellent fit of the chemical shift data results (Table III) except for phenyl. Values of “E_{cat}” = 0.026, “C_A” = 0.661, and “T_{cat}” = −0.310 result. There is no evidence of π-back-bond stabilization in the Pt–X bond for any of the animers. The data indicate that electron transfer to the animer deshields the ^{19}F, while covalent effects and to a very small extent electrostatic bonding of X to platinum shield the ^{19}F.

Table III. ^{19}F Shield in (*m*- and *p*-F-Ph)Pt$(PEt_3)_2$-X

X	$^{19}F_{expt}$	$^{19}F_{calc}$ [a]
	m-Fluorophenyl	
Cl	2.50	2.54
Br	2.34	2.20
I	2.00	2.00
CN	2.53	2.47
CH_3	4.26	4.41
C≡C	3.37	3.47
C_6H_5	3.72	4.06
	p-Fluorophenyl	
Cl	10.2	10.2
Br	10.0	9.9
I	9.7	9.7
CN	9.1	9.0
CH_3	11.7	11.6
C≡C	10.4	10.4
C_6H_5	10.9	11.3

[a] For the meta compound, all systems are given equal weight. The value of ^{19}F calculated is obtained by adding 2.0 to the shift calculated from the parameters “E_{cat}” = 0.026, “C_A” = 0.661, and “T_{cat}” = −0.310 which resulted from the fit of Δ(PtX–PtI). In the data fit ΔE_{an}, ΔC_B and ΔR_{an} values were calculated for the animers by subtracting the value of iodine from each X, e.g., $\Delta E_{an}X = E_{anX} - E_{anI}$. For the para compound, all systems are weighted the same. The ^{19}F values are obtained by adding 9.7 to Δ(PtX–PtI) value calculated with $E_{cat} = 0.074$, $C_A = 0.495$, and $T = -0.401$ and ΔE_{an}, ΔC_B, and ΔT_{an} values for the animers.

The above data set could be solved for four unknowns using

$$\delta^{19}F = \text{“}E_{cat}\text{”}E_{an} + \text{“}C_A\text{”}C_B + \text{“}T_{cat}\text{”}R_{an} + W \qquad (7)$$

where *W* would be the diamagnetic component of the shift of the animer bis(triethylphosphine)-*m*-fluorophenylplatinum and any constant contributions to all the shifts from animer binding. By fitting $\delta_X - \delta_I$ ($\Delta\delta^{19}F$), the constant *W* is eliminated and the fit done for three unknowns. The value of *W* can be determined after the fit by substituting into eq 7 the value 2.0 (the iodo shift) for δ, along with E_{an}, C_B, and R_{an} for iodide, and the “E_{cat}”, “C_A”, and “T_{cat}” from Table III. A value of $W = 0.53$ results. We are now in a position to calculate δ for the ^{19}F metal fluorophenyl with any substituent bonded to platinum by substituting the E_{an}, C_B, and R_{an} for the substituent from Table I with $W = 0.53$ into eq 7.

The bis(triethylphosphine)-*p*-fluorophenylplatinum(II) data[17] are also fit using $\Delta\delta^{19}F$ defined as $L_nPtX{-}L_nPtI$. Values of “E_{cat}” = 0.074, “C_A” = 0.495, and “T_{cat}” = −0.401 result. The shieldings of the *p*-fluoro complexes are considerably larger than those of the analogous *m*-fluoro derivative. This is understood in terms of the ionicity of the platinum–fluorophenyl bond imparting carbanion-like character to the bound carbon. This tends to decrease ring-fluorine π-bonding at the para position because C–F π-bonding places negative charge on the carbon bound to platinum:

Decreased ring–fluorine π-bonding shields the para fluoro, accounting for the large difference in the *p*- and *m*-fluoro shielding. The ^{19}F shifts can be calculated directly from the animer parameters of Table I, by substituting $W = 8.7$ into eq 4.

The next concern is how perturbations from the bound X group trans to the fluorophenyl influence the ^{19}F shielding. The meta

---

[14] Wayland, B. B.; Coffin, V. L.; Sherry, A. E.; Brennen, W. R. in ref 1b.

[15] Craig, P. J.; Green, M. *J. Chem. Soc. A* **1969**, 157.

[16] Moloy, K. G.; Marks, T. J. *J. Am. Chem. Soc.* **1984**, *106*, 7051.

[17] Parshall, G. W. *J. Am. Chem. Soc.* **1966**, *88*, 704.

position will be influenced by the partial positive charge on platinum removing electron density from the bound carbon. This effect is transmitted through the σ framework of the ring. As expected, electron transfer from platinum to X will increase the charge on the metal, deshielding the fluorine and accounting for the negative *T*. Covalent and to a very small extent electrostatic bonding to X makes the metal–fluorophenyl–platinum bond more ionic and shields the fluorine.

The *p*-fluorophenyl, though shielded considerably more than the meta isomer, only changes by 2.6 ppm as X is changed. This compares with a change of 2.3 ppm for the meta derivative. If σ-inductive effects dominate, the changes are expected to be smaller at the para position than at the meta. The slightly larger changes observed at the para indicate a small contribution from changes in the extent of ring-fluorine π-bonding. It is to be emphasized that this can occur without metal–fluorophenyl π-back-bonding by simply changing the partial charge on the carbon that is σ-bonded to platinum. The similar *E*, *C*, *T* parameters obtained for the *p*-fluoro ("*E*" = 0.074, "*C*" = 0.495, "*T*" = −0.401) and the *m*-fluoro shifts ("*E*" = 0.026, "*C*" = 0.661, "*T*" = −0.310) indicate that both substituents are responding in a similar way to changes in the platinum–X bond.

Both π-back-bonding and π-antibonding (involves lone pairs on X) interactions in the metal–ligand bond were employed[17] to interpret these shifts. The *ECT* interpretation is based only on a σ metal–X bond to interpret all the *m*-fluoro and the *p*-fluoro shifts. There is no metal-to-ligand π-back-bonding in the coordinated cyano group. This indicates that the enthalpy predicted for the (DPPE)Pt(CH_3)–CN compound is probably accurate and has no significant stabilization from π-back-bonding. Though there is no evidence of steric effects for the phenyl substituent in (DPPE)Pt, both the *m*-F and *p*-F shifts miss in this direction. Bulkier ligands are involved in the complex used in the spectral studies.

Calculations

The large number of new animers encountered in the organometallic systems encouraged us to simultaneously solve for all the new unknowns in eq 1, fixing the well-established parameters. The alternative approach would involve substituting enthalpies for systems with known animer parameters into eq 1 and solving individually for each new catimer parameters. The known catimer parameters then would be substituted into eq 1 for bonding to a new single animer and the animer parameters determined. The process could be reiterated. The fit of the entire data set was considered more direct and more accurate. The details of the least-squares minimization routine employed to fit the data have been reported.[4a] The contribution a particular bond dissociation energy makes to the final determination of the parameters is weighted according to the experimental error in the measured value as reported.[4a] In the fit reported here, systems with tentative parameters in the earlier fit, e.g., CH_3, were allowed to float in this fit with all the dissociation energies from the earlier fit added to this one. Some of the earlier animer parameters were also redetermined. Several iterations were required in which the weights of suspect systems were varied before the final fit was carried out. Given the minimum is quite shallow, the parameters for those systems that fit well and did not vary from fit to fit, e.g., chloride, were held fixed in the latter fits. This ensured staying in the same minimum. Some systems with limited data gave negative parameters. In the final data fit, these parameters were fixed at a small positive value, and all the parameters for these systems are labeled tentative. Further bond energy measurements should be designed to fill the voids in this data base. Then the fit of the combined data from here and ref 4 should lead to a well-defined minimum.

Registry No. $(CO)_5Mn^{I}-CH_3CO$, 13963-91-2; $(CO)_5Mn^{I}-CH_2C_6H_5$, 14049-86-6; $(CO)_5Mn^{I}-C_6H_5$, 13985-77-8; $(CO)_5Mn^{I}-I$, 14879-42-6; $(CO)_5Mn^{I}-CH_3$, 13601-24-6; $(CO)_5Mn^{I}-H$, 16972-33-1; $\eta^5-[(CH_3)_3SiC_5H_4]_3U^{IV}-CH_2C_6H_5$, 136912-65-7; $\eta^5-[(CH_3)_3SiC_5H_4]_3U^{IV}-CH_2CH_2CH_2CH_3$, 123383-47-1; $\eta^5-[(CH_3)_3SiC_5H_4]_3U^{IV}-I$, 123414-84-6; $\eta^5-[(CH_3)_3SiC_5H_4]_3U^{IV}-CH_3$, 123383-46-0; $\eta^5-[(CH_3)_3SiC_5H_4]_3U^{IV}-CH{=}CH_2$, 123383-51-7; $\eta^5-[(CH_3)_3SiC_5H_4]_3U^{IV}-CH_2Si(CH_3)_3$, 123383-48-2; $\eta^5-[C_5(CH_3)_5](CO)_3Mo^{II}-CH_2C_6H_5$, 96191-64-9; $\eta^5-[C_5(CH_3)_5](CO)_3Mo^{II}-CH_2CH_3$, 136893-48-6; $\eta^5-[C_5(CH_3)_5](CO)_3Mo^{II}-I$, 51213-24-2; $\eta^5-[C_5(CH_3)_5](CO)_3Mo^{II}-CH_3$, 12129-92-9; $\eta^5-[C_5(CH_3)_5](CO)_3Mo^{II}-H$, 78003-92-6; $\eta^5-[C_5(CH_3)_5](CO)_3Mo^{II}-Cl$, 63511-23-9; $\eta^5-[C_5(CH_3)_5](CO)_3Mo^{II}-Br$, 82182-11-4; $\eta^5-[C_5(CH_3)_5][P(CH_3)_3](H)Ir^{III}-C_6H_5$, 80146-02-7; $\eta^5-[C_5(CH_3)_5][P(CH_3)_3](H)Ir^{III}-CH_2CH_2CH_2CH_3$, 96096-97-8; $\eta^5-[C_5(CH_3)_5][P(CH_3)_3](H)Ir^{III}-I$, 136893-49-7; $\eta^5-[C_5(CH_3)_5][P(CH_3)_3](H)Ir^{III}-CH_3$, 88548-54-3; $\eta^5-[C_5(CH_3)_5][P(CH_3)_3](H)Ir^{III}-H$, 80146-01-6; $\eta^5-[C_5(CH_3)_5][P(CH_3)_3](H)Ir^{III}-Cl$, 80303-34-0; $\eta^5-[C_5(CH_3)_5][P(CH_3)_3](H)Ir^{III}-Br$, 136893-50-0; $\eta^5-[C_5(CH_3)_5][P(CH_3)_3](H)Ir^{III}-CH{=}CH_2$, 97135-44-9; $\eta^5-[C_5(CH_3)_5]_2[(CH_3)_3CO]Th^{IV}-CH_2CH_3$, 136893-51-1; $\eta^5-[C_5(CH_3)_5]_2[(CH_3)_3CO]Th^{IV}-C_6H_5$, 110487-78-0; $\eta^5-[C_5(CH_3)_5]_2[(CH_3)_3CO]Th^{IV}-CH_2CH_2CH_2CH_3$, 127087-56-3; $\eta^5-[C_5(CH_3)_5]_2[(CH_3)_3CO]Th^{IV}-CH_3$, 79301-34-1; $\eta^5-[C_5(CH_3)_5]_2[(CH_3)_3CO]Th^{IV}-H$, 79301-35-2; $\eta^5-[C_5(CH_3)_5]_2[(CH_3)_3CO]Th^{IV}-CH_2Si(CH_3)_3$, 136893-52-2; $\eta^5-[C_5(CH_3)_5][P(CH_3)_3]_2Ru^{II}-CH_2CH_3$, 87640-50-4; $\eta^5-[C_5(CH_3)_5][(CH_3)_3]_2Ru^{II}-C_6H_5$, 107441-17-8; $\eta^5-[C_5(CH_3)_5][P(CH_3)_3]_2Ru^{II}-CH_3$, 87640-49-1; $\eta^5-[C_5(CH_3)_5][P(CH_3)_3]_2Ru^{II}-H$, 87640-53-7; $\eta^5-[C_5(CH_3)_5][P(CH_3)_3]_2Ru^{II}-CH_2Si(CH_3)_3$, 87640-52-6; $\eta^5-[C_5(CH_3)_5][P(CH_3)_2]_2Ru^{II}-OH$, 106734-52-5; $\eta^5-[C_5(CH_3)_5][P(CH_2)_3]_2Ru^{II}-C{\equiv}CC_6H_5$, 106734-53-6; $\eta^5-[C_5(CH_3)_5][P(CH_3)_3]Ru^{II}-CH_2COCH_3$, 106734-54-7; $\eta^5-[C_5(CH_3)_5][P(CH_3)_3]_2Ru^{II}-OCH_3$, 106734-58-1; $\eta^5-[C_5(CH_3)_5][P(CH_3)_3]_2Ru^{II}-CN$, 91993-49-6; $\eta^5-[C_5(CH_3)_5][P(CH_3)_3]_2Ru^{II}-SH$, 106734-57-0; $[(C_6H_5)_2PCH_2CH_2P(C_6H_5)_2](CH_3)Pt^{II}-CH_2CH_3$, 136893-53-3; $[(C_6H_5)_2PCH_2CH_2P(C_6H_5)_2](CH_3)Pt^{II}-C_6H_5$, 52595-93-4; $[(C_6H_5)_2PCH_2CH_2P(C_6H_5)_2](CH_3)Pt^{II}-CH_3$, 15630-18-9; $[(C_6H_5)_2PCH_2CH_2P(C_6H_5)_2](CH_3)Pt^{II}-H$, 76125-11-6; $[(C_6H_5)_2PCH_2CH_2P(C_6H_5)_2](CH_3)Pt^{II}-CH_2Si(CH_3)_3$, 136893-54-4; $[(C_6H_5)_2PCH_2CH_2P(C_6H_5)_2](CH_3)Pt^{II}-OH$, 43210-95-3; $[(C_6H_5)_2PCH_2CH_2P(C_6H_5)_2](CH_3)Pt^{II}-C{\equiv}CC_6H_5$, 65310-61-4; $[(C_6H_5)_2PCH_2CH_2P(C_6H_5)_2](CH_3)Pt^{II}-CH_2COCH_3$, 43210-96-4; $[(C_6H_5)_2PCH_2CH_2P(C_6H_5)_2](CH_3)Pt^{II}-OCH_3$, 82405-05-8; $[(C_6H_5)_2PCH_2CH_2P(C_6H_5)_2](CH_3)Pt^{II}-CN$, 65310-86-3; $[(C_6H_5)_2PCH_2CH_2P(C_6H_5)_2](CH_3)Pt^{II}-SH$, 65310-84-1; $\eta^5-[C_5(CH_3)_5]_2Sm-I$, 122213-83-6; $\eta^5-[C_5(CH_3)_5]_2Sm-H$, 136893-55-5; $\eta^5-[C_5(CH_3)_5]_2Sm-Cl$, 136893-56-6; $\eta^5-[C_5(CH_3)_5]_2Sm-Br$, 122213-89-2; $\eta^5-[C_5(CH_3)_5]_2Sm-CH_2Si(CH_3)_3$, 136893-57-7; $\eta^5-[C_5(CH_3)_5]_2Sm-OCH_3$, 136893-58-8; $\eta^5-[C_5(CH_3)_5]_2Sm-SCH_3$, 136893-59-9; $\eta^5-[C_5(CH_3)_5]_2Sm-N(CH_3)_2$, 122213-87-0; $\eta^5-[C_5(CH_3)_5]_2Zr-I$, 136893-60-2; $\eta^5-[C_5(CH_3)_5]_2Zr-CH_3$, 136893-61-3; $\eta^5-[C(CH_3)_5]_2Zr-H$, 136893-62-4; $\eta^5-[C_5(CH_3)_5]_2Zr-Cl$, 136893-63-5; $\eta^5-[C_5(CH_3)_5]_2Zr-Br$, 136893-64-6; (*m*-F-Ph)Pt$(PEt_3)_2$-Cl, 14494-23-6; (*m*-F-Ph)Pt$(PEt_3)_2$-Br, 136983-06-7; (*m*-F-Ph)Pt$(PEt_3)_2$-I, 136983-07-8; (*m*-F-Ph)Pt$(PEt_3)_2$-CN, 136983-08-9; (*m*-F-Ph)Pt$(PEt_3)_2$-CH_3, 136983-09-0; (*m*-F-Ph)Pt$(PEt_3)_2$-$C{\equiv}CC_6H_5$, 15670-83-4; (*m*-F-Ph)Pt$(PEt_3)_2$-C_6H_5, 136983-10-3; (*p*-F-Ph)Pt$(PEt_3)_2$-Cl, 14494-23-6; (*p*-F-Ph)Pt$(PEt_3)_2$-Br, 136983-11-4; (*p*-F-Ph)Pt$(PEt_3)_2$-I, 136983-12-5; (*p*-F-Ph)Pt$(PEt_3)_2$-CN, 100017-33-2; (*p*-F-Ph)Pt$(PEt_3)_2$-CH_3, 136983-13-6; (*p*-F-Ph)Pt$(PEt_3)_2C{\equiv}CC_6H_5$, 15670-84-5; (*p*-F-Ph)Pt$(PEt_3)_2$-C_6H_5, 136983-14-7.

Supplementary Material Available: Data for *ECT* fit for use in eq 1 (13 pages). Ordering information is given on any current masthead page.